Blocking Artifact Detection and Reduction in Compressed Data

George A. Triantafyllidis, *Student Member, IEEE*, Dimitrios Tzovaras, and Michael Gerassimos Strintzis, *Senior Member, IEEE*

***Abstract*—A novel frequency-domain technique for image blocking artifact detection and reduction is presented in this paper. The algorithm first detects the regions of the image which present visible blocking artifacts. This detection is performed in the frequency domain and uses the estimated relative quantization error calculated when the discrete cosine transform (DCT) coefficients are modeled by a Laplacian probability function. Then, for each block affected by blocking artifacts, its dc and ac coefficients are recalculated for artifact reduction. To achieve this, a closed-form representation of the optimal correction of the DCT coefficients is produced by minimizing a novel enhanced form of the mean squared difference of slope for every frequency separately. This correction of each DCT coefficient depends on the eight neighboring coefficients in the subband-like representation of the DCT transform and is constrained by the quantization upper and lower bound. Experimental results illustrating the performance of the proposed method are presented and evaluated.**

***Index Terms*—Blocking artifacts, compressed domain, MSDS metric.**

I. Introduction

THE BLOCK-based discrete cosine transform (B-DCT) scheme is a fundamental component of many image and video compression standards including JPEG [1], [2], H.263 [3], MPEG-1, MPEG-2, MPEG-4 [4], and others, used in a wide range of applications. The B-DCT scheme takes advantage of the local spatial correlation property of the images by dividing the image into 8×8 blocks of pixels, transforming each block from the spatial domain to the frequency domain using the discrete cosine transform (DCT) and quantizing the DCT coefficients. Since blocks of pixels are treated as single entities and coded separately, correlation among spatially adjacent blocks is not taken into account in coding, which results in block boundaries being visible when the decoded image is reconstructed. For example, a smooth change of luminance across a border can result in a step in the decoded image if neighboring samples fall into different quantization intervals. Such so-called "blocking" artifacts are often very disturbing, especially when the transform coefficients are subject to coarse quantization.

Subjective picture quality can be significantly improved by decreasing the blocking artifacts. Increasing the bandwidth or bit rate to obtain better quality images is often not possible or is too costly. Other approaches to improve the subjective quality of the degraded images have been published. Techniques which do not require changes to existing standards appear to be the most practical solution, and with the fast increase of available computing power, more sophisticated methods can be implemented. If the blocking effects can be significantly reduced, a higher compression ratio can be achieved.

In this paper, a new method is proposed for the detection and reduction of the blocking effects in the B-DCT. First, blocks which show blocking artifacts with the neighboring blocks are detected. The detection scheme is applied in the subband-like representation of the modified DCT coefficients which are produced, if we assume that the DCT coefficients follow the Laplacian probability model [37] (hereafter, Laplacian corrected DCT coefficients). Specifically, the presence of visual blocking artifacts of the B-DCT reconstructed image is inferred from data in the frequency domain. Then, the blockiness is assumed when the relative difference of two neighboring Laplacian corrected DCT coefficients in the subband-like domain is greater than a threshold.

For every block found to present blocking artifacts, the lowest frequency DCT coefficients are recalculated by minimizing a novel enhanced form of the mean squared difference of slope (MSDS) [33], which involves all eight neighboring blocks. The minimization is constrained by the quantization bounds and is performed for every frequency separately, in the subband-like representation of the DCT transform. Thus, a closed-form representation is derived, which predicts the DCT coefficients in terms of the eight neighboring coefficients in the subband-like domain.

A first major advantage of the proposed algorithm is that it is applied entirely in the compressed domain. This is in contrast to the large majority of the deblocking algorithms which are applied in the spatial domain.

Compared to other methods of deblocking in the frequency domain:

- the proposed algorithm introduces the novel and enhanced form of MSDS_t which involves all neighboring blocks, including the diagonally located neighboring blocks;
- our algorithm minimizes MSDS_t in the frequency domain, in order to recalculate the DCT coefficients for blockiness removal. This minimization is performed

Manuscript received May 11, 2000; revised March 20, 2002. This work was supported by the IST European Project OTELO. This paper was recommended by Associate Editor O. K. Al-Shaykh.

G. A. Triantafyllidis is with the Information Processing Laboratory, Aristotle University of Thessaloniki, Thessaloniki 54006, Greece (e-mail: gatrian@iti.gr).

D. Tzovaras is with the Informatics and Telematics Institute, Thessaloniki 546 39, Greece (e-mail: Dimitrios.Tzovaras@iti.gr).

M. G. Strintzis is with the Information Processing Laboratory, Aristotle University of Thessaloniki, Thessaloniki 54006, Greece, and also with the Informatics and Telematics Institute, Thessaloniki 546 39, Greece (e-mail: strintzi@eng.auth.gr).

Digital Object Identifier 10.1109/TCSVT.2002.804880

for each frequency separately, producing better results than global minimization. This is intuitively expected because B-DCT schemes (such as JPEG) use scalar rather than vector quantization, and also, the DCT transform (which is an approximation of the Karhuene–Loeve (KL) transform) produces almost uncorrelated coefficients';
- furthermore, this paper contains the novel proposition that the Laplacian corrected DCT coefficients should be used in place of the simple DCT reconstructed coefficients in the formula which provides the correction of the DCT coefficients, because they provide statistically better estimates of the original DCT coefficients. This proposition is supported by the experimental results;
- finally, this paper presents not only a method for the removal of the blocking artifacts, but also proposes a novel blockiness detection method which reduces the time and the computational load of deblocking algorithms by having the deblocking algorithm applied only where needed (where there exist disturbing blocking artifacts).

The rest of this paper is organized as follows. In Section II, a review and discussion of various techniques that have been proposed in the past for the removal of blocking artifacts are given. Section III describes the mathematical analysis underlying the concept of blocking artifact detection in the subband-like transform domain, under the assumption that the DCT transform follows a Laplacian probability density function (pdf). Section IV presents in detail the blocking artifact reduction algorithm by constrained minimization. Experimental results given in Section V evaluate visually and quantitatively the performance of the proposed methods. Finally, conclusions are drawn in Section VI.

II. Background

Many techniques have been proposed in the literature for the reduction of blocking artifacts. Two general approaches have been followed. In the first approach, the blocking effect is dealt with at the encoding side [5], [6]. The second approach proposes postprocessing at the decoding side, aiming to improve the visual quality of the reconstructed image without any modification on the encoding or decoding procedures. Due to this advantage, most of the recently proposed algorithms follow the second approach.

The majority of the postprocessing techniques in the literature are applied in the spatial domain. These techniques may be classified into several categories: 1) the spatial filtering methods [7]–[10]; 2) methods based on wavelet representation [11]–[14]; 3) MRF approaches [15]–[17]; and 4) the iterative regularization restoration approaches [18]–[21].

In the first category, Jarske *et al.* [7] test several filters to conclude that the Gaussian low-pass filter with a high-pass frequency emphasis gives the best performance. Reeves and Lim [8] apply the 3×3 Gaussian filter only to those pixels along block boundaries. A similar technique by Tzou [22] applies a separable anisotropic Gaussian filter, such that the primary axis of the filter is always perpendicular to the block boundary. A space-variant filter that adapts to local characteristics of the signal is proposed by Ramamurthi and Gersho in [23]. The algorithm distinguishes edge pixels from nonedge pixels via a neighborhood testing and then switches between a one–dimensional (1-D) and a two–dimensional (2-D) filter accordingly to reduce blocking effects. In [24], an adaptive filtering scheme is reported, progressively transforming a median filter within blocks to a low-pass filter when it approaches the block boundaries. An adaptive filtering process is also employed in [25]. The shape and the position of the Gaussian filtering are adjusted based on an estimation of the local characteristics of the coded image. A region-based method is presented in [9], where the degraded image is segmented by a region growing algorithm, and each region obtained by the segmentation is enhanced separately by a Gaussian low-pass filter. Lee *et al.* in [26] propose a 2-D signal-adaptive filtering and Chou *et al.* [27] remove blockiness by performing a simple nonlinear smoothing of pixels. In [10], Apostolopoulos *et al.* propose to identify the blocks that potentially exhibit blockiness by calculating the number of nonzero DCT coefficients in a coded block and comparing it to a threshold. Then, a filter is applied along the boundaries but only updating the pixels within the distorted block. However, the above filtering approaches frequently result in overblurred recovered images, especially at low bit rates. Another approach is proposed in [28]–[30], where the optimal filters for subband coding of the quantized image are efficiently determined for the reduction of quantization effects in low bit rates.

In the second category, Xiong *et al.* [12] use an overcomplete wavelet representation to reduce the quantization effects of block based DCT. Other approaches using wavelet representation are presented in [11], [13], and [14]. In [14] the wavelet transform modulus maxima (WTMM) representation is used for efficient image deblocking.

In the third category, O' Rourke and Stevenson [15] propose a postprocessor that can remove blockiness in block encoded images. To achieve this, they maximize the *a posteriori* probability (MAP) of the unknown image. The probability function of the decompressed image is modeled by an MRF, and the Huber minimax function is chosen as a potential function. A similar approach is followed by Luo *et al.* [16]. In [17], Meier *et al.* remove blocking artifacts by first segmenting the degraded image into regions by an MRF segmentation algorithm, and then each region is enhanced separately using an MRF model.

Finally, in the fourth category, iterative image recovery methods using the theory of projections onto convex sets (POCS) are proposed in [19], [31], [32]. In the POCS-based method, closed convex constraint sets are first defined that represent all of the available data on the original uncoded image. Then, alternating projections onto these convex sets are iteratively computed to recover the original image from the coded image. POCS is effective in eliminating blocking artifacts but less practical for real time applications, since the iterative procedure adopted increases the computation complexity. In [18] and [21], the constrained least-square method is proposed, which aims to reconstruct the image by minimizing an objective function reflecting a smoothness property.

Very few approaches in the literature have tackled the problem of blocking artifact reduction in the transform domain [33], [34]. In the JPEG standard [1], a method for suppressing the block to block discontinuities in smooth areas of the image is introduced. It uses dc values from current and neighboring

blocks for interpolating the first few ac coefficients into the current block. In [33], Minami and Zakhor present a new approach for reducing the blocking effect. A new criterion, the mean squared difference of slope (MSDS)—a measure of the impact of blocking effects—is introduced. It is shown that the expected value of the MSDS increases after quantizing the DCT coefficients. This approach removes the blocking effect by minimizing the MSDS, while imposing linear constraints corresponding to quantization bounds. To minimize the MSDS, a quadratic programming (QP) problem is formulated and solved using a gradient projection method. The solution is obtained in the form of the optimized value of the three lowest DCT coefficients. The blocking effect due to the quantization of low frequency coefficients is reduced if the quantized DCT is replaced by the optimized values during the decoding phase. To remove the high-frequency blocking effect, low-pass filtering of the decoded image is proposed. In [34], Lakhani and Zhong follow the approach proposed in [33] for reducing blocking effects using, however, a different solution of the optimization problem, minimizing the MSDS globally and predicting the four lowest DCT coefficients.

Our proposed method for the reduction of blocking artifacts also adopts the criterion of MSDS. However, the form of MSDS which is now used has been enhanced by also involving the diagonal neighboring pixels. Furthermore, the optimization is performed in the subband-like domain for each frequency separately using the Laplacian corrected DCT coefficients. Before applying the blockiness reduction algorithm, a method is used for the detection of the most disturbing blocking artifacts in the reconstructed image. This method of blockiness detection is elaborated in the next section.

III. Detection of Blocking Artifacts Using the DCT Laplacian Model in the Subband-Like Domain

In the classical B-DCT formulation, the input image is first divided into 8 × 8 blocks, and the 2-D DCT of each block is determined. The 2-D DCT can be obtained by performing a 1-D DCT on the columns and a 1-D DCT on the rows. The DCT coefficients of the spatial block $B_{i,j}$ are then determined by the following formula:

$$F_{ij}^{D}(u, v) = C(u)C(v)\left[\sum_{n=0}^{7}\sum_{m=0}^{7} f_{ij}(n, m)\cos\frac{(2n+1)u\pi}{16} \cdot \cos\frac{(2m+1)v\pi}{16}\right],$$
$$u, v = 0,\ldots,7,\ i = 0,\ldots,\frac{N}{8}-1,\ j = 0,\ldots,\frac{M}{8}-1 \quad (1)$$

where $F_{ij}^{D}(u, v)$ are the DCT coefficients of the $B_{i,j}$ block, $f_{ij}(n, m)$ is the luminance value of the pixel (n, m) of the $B_{i,j}$ block, $N \times M$ are the dimensions of the image, and

$$C(u) = \begin{cases} \dfrac{1}{\sqrt{2}}, & \text{if } u = 0 \\ 1, & \text{if } u \neq 0. \end{cases} \quad (2)$$

The transformed output from the 2-D DCT is ordered so that the dc coefficient $F_{ij}^{D}(0, 0)$ is in the upper-left corner and the higher frequency coefficients follow, depending on their distance from the dc coefficient. The higher vertical frequencies are represented by higher row numbers and the higher horizontal frequencies are represented by higher column numbers.

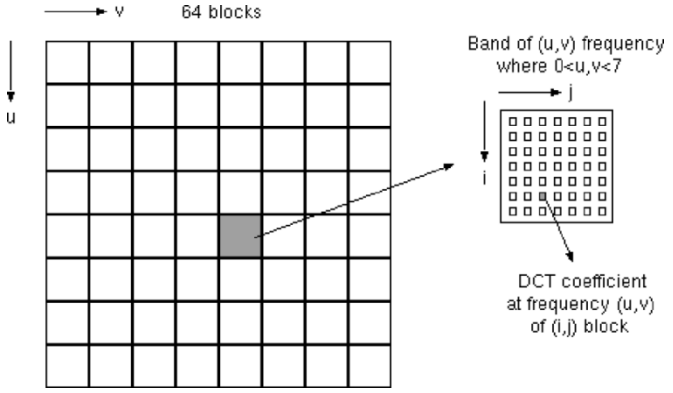

Fig. 1. Subband-like domain of DCT coefficients.

A typical quantization-reconstruction process of the DCT coefficients as described in JPEG [1] is given by

$$F_{ij}^{Q}(u, v) = round\left(\frac{F_{ij}^{D}(u, v)}{Q(u, v)}\right) \quad (3)$$

$$F_{ij}^{R}(u, v) = F_{ij}^{Q}(u, v)Q(u, v) \quad (4)$$

where $Q(u, v)$ indicates the quantization width bin for the given coefficient, $F_{ij}^{Q}(u, v)$ indicates the bin index in which the coefficient $F_{ij}^{D}(u, v)$ falls, and $F_{ij}^{R}(u, v)$ represents the reconstructed quantized coefficient. Then, the reconstructed pixel intensity is obtained from the inverse DCT.

DCT coefficients with the same frequency index (u, v) from all DCT transformed blocks can be scanned and grouped together, starting from the dc coefficients $(u = 0, v = 0)$. Thus, transforming an image with an 8 × 8 2-D DCT can be seen to produce hierarchical data equivalent to those produced by a subband transform of 64 frequency bands. Fig. 1 shows the scheme of the subband-like transform domain and Fig. 2 shows the DCT coefficients reallocated to form a subband-like transform of the image "Lena."

We shall assume that for typical input image statistics, the DCT coefficients may be reasonably modeled by a Laplacian pdf as [35]

$$f(x) = \frac{a}{2}e^{-a|x|} \quad (5)$$

which is a zero-mean pdf with variance

$$\sigma^2 = 2a^2. \quad (6)$$

If the Laplacian-modeled variable is quantized using uniform step sizes, the only information available to the receiver is that the original DCT coefficient is in the interval

$$\gamma - t \leq F_{ij}^{D}(u, v) \leq \gamma + t,$$
$$\text{where } \gamma = F_{ij}^{Q}(u, v)Q(u, v) \text{ and } t = Q(u, v)/2. \quad (7)$$

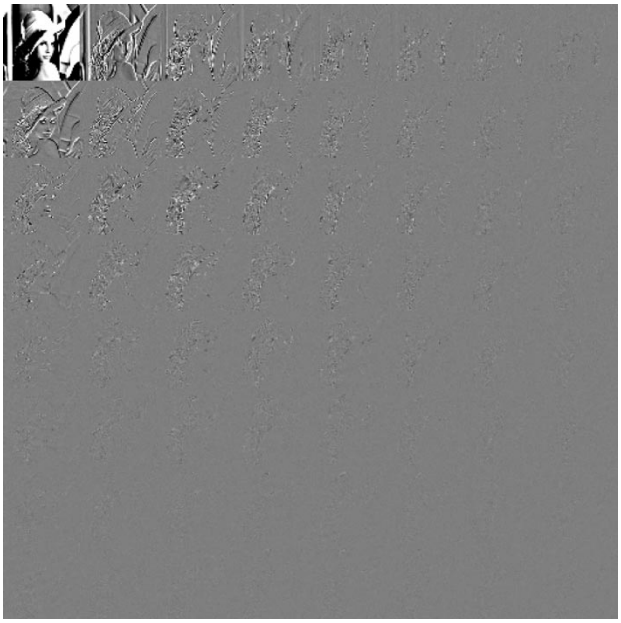

Fig. 2. Subband-like domain of DCT coefficients of "Lena" image.

The trivial solution suggested in JPEG is to reconstruct the coefficient in the center of the interval as $F_{ij}^R(u, v) = \gamma$, which simplifies implementation. The optimal reconstruction (minimum mean squared error) lies in the centroid of the distribution for the interval $(\gamma - t, \gamma + t)$, thus, under the assumption of Laplacian statistics [36], we have the following:

$$\gamma' = \frac{\int_{\gamma-t}^{\gamma+t} \lambda f(\lambda)\, d\lambda}{\int_{\gamma-t}^{\gamma+t} f(\lambda)\, d\lambda} = \gamma + \frac{1}{a} - t\coth(at). \tag{8}$$

Note that this implies a bias δ toward the origin

$$\delta = \gamma - \gamma' = t\coth(at) - \frac{1}{a}. \tag{9}$$

For different coefficients, we have different step sizes and variances [37]. Therefore, considering the DCT coefficient of block $B_{i,j}$ at frequency (u, v), we have quantization step size $Q(u, v)$ and variance $\sigma_{ij}^2(u, v)$. Then, the bias δ_{ij}^{uv} toward the origin can be found from (9) and (7)

$$\delta_{ij}^{uv} = \frac{Q(u, v)}{2}\coth\left(\frac{a_{ij}(u, v)Q(u, v)}{2}\right) - \frac{1}{a_{ij}(u, v)}. \tag{10}$$

Given the coefficient variances, we can estimate the a parameters using (6), thus $a_{ij}(u, v) = \sqrt{2}/\sigma_{ij}(u, v)$. The variances can be easily estimated by $\sigma_{ij}^2(u, v) = [F_{ij}^R(u, v)]^2$ [38]. This estimation is only used for the calculation of δ_{ij}^{uv} and employs the reconstructed DCT coefficients in place of the original DCT coefficients, since only the former coefficients are available.

Alternatively, we may estimate $\sigma_{ij}^2(u, v)$ in the way proposed in [40], which estimates the variances of the DCT coefficients from the variances of the pixel values using the form

$$\sigma_F^2(u, v) = \sigma_f^2 \begin{bmatrix} 9.756 & 5.5505 & \cdots & 0.7971 \\ 5.5505 & 3.2513 & \cdots & \\ \cdots & \cdots & & \\ 0.7971 & \cdots & & 0.0671 \end{bmatrix}. \tag{11}$$

Experiments have shown that the results are very similar to those of the adopted method, described earlier. However, we did not choose to employ the method in [40] because it is more computationally inefficient.

Therefore, we can use (9) to precalculate all δ_{ij}^{uv} so as to obtain the optimal estimation $\hat{F}_{ij}^R(u, v)$ of the reconstructed DCT coefficient (Laplacian corrected DCT coefficients)

$$\begin{aligned}\hat{F}_{ij}^R(u, v) &= F_{ij}^R(u, v) - sign\left[F_{ij}^Q(u, v)\right]\delta_{ij}^{uv} \\ &= F_{ij}^Q(u, v)Q(u, v) - sign\left[F_{ij}^Q(u, v)\right]\delta_{ij}^{uv}\end{aligned} \tag{12}$$

where the $sign$ function is appropriately used to handle both positive and negative values and $sign[0] = 0$.

The above concepts are now extended and applied to define a method for blockiness detection. First, we define the newly introduced relative theoretical quantization error e_{ij}^{uv} for coefficient $F_{ij}^R(u, v)$ by

$$e_{ij}^{uv} = \frac{\hat{F}_{ij}^R(u, v) - F_{ij}^R(u, v)}{F_{ij}^R(u, v)}. \tag{13}$$

We next focus on the difference $|e_{ij}^{uv} - e_{kl}^{uv}|$ between the B_{ij} and B_{kl} blocks. Occurrences of large values of this difference indicate that very different levels were used to quantize the B_{ij} and B_{kl} blocks, producing a blocking artifact between these blocks. Thus, we shall infer the presence of an artifact between blocks B_{ij} and B_{kl} if

$$\left|e_{ij}^{uv} - e_{kl}^{uv}\right| > T_{ijkl}^{uv} \tag{14}$$

where T_{ijkl}^{uv} is an adaptive threshold defined by

$$T_{ijkl}^{uv} = \frac{\hat{F}_{ij}^R(u, v) - \hat{F}_{kl}^R(u, v)}{F_{ij}^R(u, v) - F_{kl}^R(u, v)}. \tag{15}$$

For a given compressed image, the detection criterion is applied on each coefficient in all of the 64 bands of the DCT subband-like domain, in order to locate the most disturbing blocking artifacts. More specifically, for each band in the subband-like domain, we scan the coefficients vertically, horizontally and diagonally, and apply criterion (14). We assume that a blocking artifact between the (i, j) block and the neighboring (k, l) block is disturbing when (14) is satisfied for more than two frequencies in the subband-like domain, e.g., (u, v) and (q, r) frequencies. Thus, we introduce the following criterion:

$$\begin{aligned}&\text{Artifact between neighboring blocks } B_{ij} \text{ and } B_{kl} \\ &\text{if } \exists \text{ frequencies } (u, v), (q, r) \text{ that } |e_{ij}^{uv} - e_{kl}^{uv}| > T_{ijkl}^{uv} \\ &\qquad \text{and } |e_{ij}^{qr} - e_{kl}^{qr}| > T_{ijkl}^{qr}.\end{aligned} \tag{16}$$

This criterion was tested in a large number of pictures and was found to be very efficient in detecting the most disturbing blocking artifacts.

IV. Reduction of Blocking Artifact in the Frequency Domain

As noted, blocking effects result in discontinuities across block boundaries. Based on this observation, a metric called

MSDS was introduced in [33], involving the intensity gradient (slope) of the pixels close to the boundary of two blocks. Specifically, it is based on the empirical observation that quantization of the DCT coefficients of two neighboring blocks increases the MSDS between the neighboring pixels on their boundaries.

To better understand this metric, consider an 8×8 block f of the input image and a block w horizontally adjacent to f. If the coefficients of the adjacent blocks are coarsely quantized, a difference in the intensity gradient across the block boundary is expected. This abrupt change in intensity gradient across the block boundaries of the original unquantized image is rather unlikely, because most parts of most natural images can be considered to be smoothly varying and their edges are unlikely to line up with block boundaries. From the above, it is clear that a reasonable method for the removal of the blocking effects is to minimize the MSDS, which is defined by

$$\varepsilon_w = \sum_{m=0}^{7} [d_1(m) - d_2(m)]^2 \tag{17}$$

where $d_1(m)$ is the intensity slope across the boundary between the f and w blocks, defined by

$$d_1(m) = f(m, 0) - w(m, 7) \tag{18}$$

and $d_2(m)$ is the average between the intensity slope of f and w blocks close to their boundaries, defined by

$$d_2(m) = \frac{w(m, 7) - w(m, 6)}{2} + \frac{f(m, 1) - f(m, 0)}{2}. \tag{19}$$

The ideas in the above discussion are applicable to both horizontal and vertical neighboring blocks. Specifically, if blocks w, e denote the blocks horizontally adjacent to f, and blocks s, n present the blocks vertically adjacent to f, then, the MSDS which involves both horizontal and vertical adjacent blocks (hereafter, MSDS_1) is given by

$$\text{MSDS}_1 = \varepsilon_w + \varepsilon_e + \varepsilon_s + \varepsilon_n \tag{20}$$

where ε_e, ε_s and ε_n are defined similarly to (17)–(19).

We now extend the definition of MSDS by involving the four diagonally adjacent blocks. If nw is a block diagonally adjacent to f, then we define

$$\varepsilon_{nw} = [g_1 - g_2]^2 \tag{21}$$

where

$$g_1 = f(0, 0) - nw(7, 7)$$

and

$$g_2 = \frac{nw(7, 7) - nw(6, 6)}{2} + \frac{f(1, 1) - f(0, 0)}{2}. \tag{22}$$

If nw, ne, sw, and se are the four blocks diagonally adjacent to f; the MSDS involving only the diagonally adjacent blocks (hereafter, MSDS_2) is

$$\text{MSDS}_2 = \varepsilon_{nw} + \varepsilon_{ne} + \varepsilon_{sw} + \varepsilon_{se} \tag{23}$$

where ε_{ne}, ε_{sw}, and ε_{se} are defined in a manner similar to (21) and (22). Thus, the total MSDS (hereafter, MSDS_t) considered in this paper, involving the intensity slopes of all the adjacent blocks is

$$\text{MSDS}_t = \text{MSDS}_1 + \text{MSDS}_2. \tag{24}$$

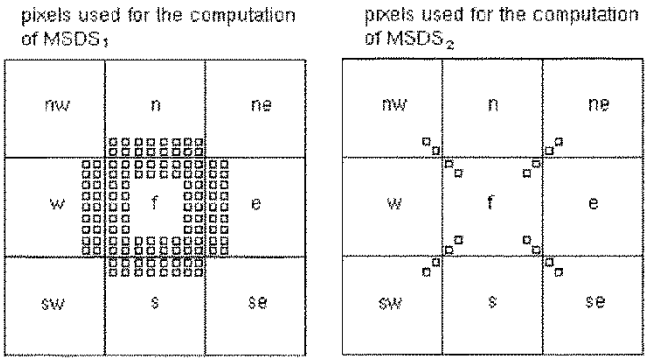

Fig. 3. Vertical and horizontal slope (MSDS_1) and diagonal slope (MSDS_2).

Fig. 3 shows the pixels involved in the calculation of MSDS_1 and MSDS_2.

The form of MSDS used in the proposed methods of [33] and [34] is MSDS_1 which, as mentioned above, involves only the horizontal and vertical adjacent blocks for its computation and thus does not use the intensity slopes of the four diagonally adjacent blocks. This implies that their methods cannot remove the specific type of blocking artifact called "corner outlier" [26], which may appear in a corner point of the 8×8 block. Moreover, even if we ignore the reduction of the corner outliers, the introduction of the MSDS_t yields better results than the simple form of MSDS_1, since more neighboring pixels (i.e., the neighboring diagonal pixels) are used, providing a better estimation for the DCT recalculation.

In [34], a global minimization of the MSDS_1 is proposed for the reduction of blocking effects. However, since B-DCT schemes (such as JPEG) use scalar quantization (i.e., quantization of individual samples) for each frequency separately, a separate minimization of the contribution of the quantization of each particular coefficient to the blocking artifact is more appropriate than a global minimization. Global minimization would be more suitable if vector quantization (i.e., quantization of groups of samples or vectors) of the DCT coefficients were used, which is, however, not the case in B-DCT coding schemes. Consider also that, since the DCT transform is very close to the KL transform, the DCT coefficients are almost uncorrelated [41]. Thus, the modification of each DCT coefficient based on the minimization of MSDS which includes values of the low-, middle-, and high-pass frequency coefficients is obviously not the best solution, and the minimization of MSDS_t for each frequency separately is the appropriate procedure.

The new enhanced form of the MSDS_t involving all eight neighboring blocks is used in this paper, and its local constrained minimization for each frequency, produces a closed-form representation for the correction of the DCT coefficients in the subband-like domain of the DCT transform. To achieve this, the form of MSDS_t in the frequency domain is obtained, and all other frequencies apart from the one (k, l) under consideration are set to zero. It was observed that only

the first sixteen DCT coefficients (i.e., $0 \le k, l \le 4$) need to be recalculated by MSDS minimization, since the modification of the remaining coefficients does not improve significantly the reduction of the blocking artifacts (because of their poor contribution to MSDS [34]), while requiring noneligible extra computational load. In the sequel, the MSDS_t is calculated and minimized in the frequency domain.

A. Calculation of $MSDS_1$ in the Frequency Domain

Let $f(m, n)$ denote a 8×8 block of the input image and $F(u, v)$ denote its forward DCT, where $0 \le m, n, u, v \le 7$ and (0, 0) denotes the upper-left corner pixel of the block as well as the first (dc) transform coefficient. Let w, n, e, s, nw, ne, sw, and se denote the eight blocks adjacent to f in the horizontal, vertical, and diagonal directions, and W, N, E, S, NW, NE, SW, and SE denote their corresponding forward DCTs.

Following (18) and (19), the expression $d_1(m) - d_2(m)$ which is used for the calculation of ε_w in (17) is

$$d_1(m) - d_2(m) = f(m, 0) - w(m, 7) - \left(\frac{w(m, 7) - w(m, 6)}{2} + \frac{f(m, 1) - f(m, 0)}{2}\right) \quad (25)$$

where $0 \le m \le 7$.

Let G denote the discrete cosine transformation matrix [where the uth row of G is the basis vector $C(u)\cos((2m + 1)u\pi/16)$] and G^T denote its transpose. Then, the f block can be derived from the inverse DCT transform as follows:

$$\text{Inverse DCT: } f = G^T F G. \quad (26)$$

Let G_x and G^y denote the xth row and yth column of the discrete cosine transformation matrix G. Using (26), $f(m, 0)$ is easily seen to equal $G_m^T F G^0$. Likewise, the other terms of (25) can also be expressed in the frequency domain and (25) can be expressed as follows:

$$d_1(m) - d_2(m) = \left(G_m^T F G^0 - G_m^T W G^7\right) - \left(\frac{G_m^T W G^7 - G_m^T W G^6}{2} + \frac{G_m^T F G^1 - G_m^T F G^0}{2}\right). \quad (27)$$

Since

$$G^1 = (-1)^u G^6 \quad \text{and} \quad G^0 = (-1)^u G^7 \quad (28)$$

where u denotes the row number and $0 \le u \le 7$, expression (27) reduces to

$$\begin{aligned} &d_1(m) - d_2(m) \\ &= (1/2) G_m^T \left(3FG^0 - 3W(-1)^u G^0 - FG^1 + W(-1)^u G^1\right) \\ &= (1/2) G_m^T (F - (-1)^u W)\left(3G^0 - G^1\right). \end{aligned} \quad (29)$$

Since G is a unitary orthogonal transform, then $\sum_{m=0}^{7} G^m G_m^T = I$, where I is the identity matrix. Thus, adding the squares of (29) for all m according to (17), the MSDS term ε_w between the f and w blocks is produced

$$\varepsilon_w = (1/4)\left(3G_0^T - G_1^T\right)(F - (-1)^u W)^T \cdot (F - (-1)^u W)\left(3G^0 - G^1\right). \quad (30)$$

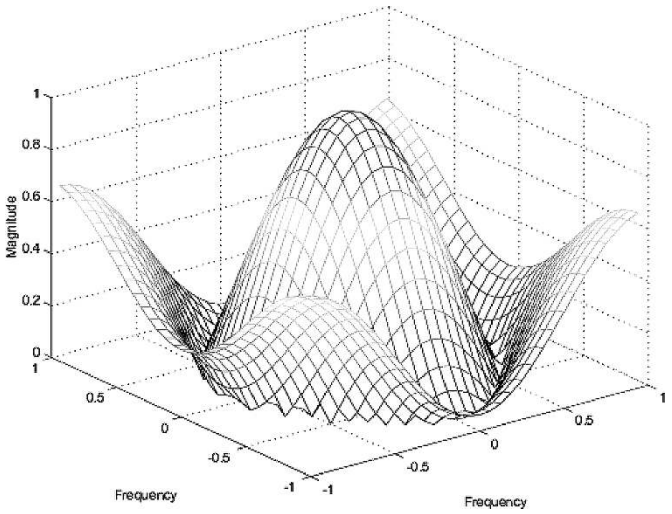

Fig. 4. Frequency response of the filter derived by the proposed method for the frequencies $(k, l) = 2, 3$.

The sum of the MSDS terms of the f block corresponding to the four horizontally and vertically adjacent blocks can now be expressed as [34]

$$\begin{aligned} \text{MSDS}_1 &= \varepsilon_w + \varepsilon_e + \varepsilon_s + \varepsilon_n \\ &= (1/4)\left(3G_0^T - G_1^T\right)\left[(F - (-1)^u W)^T (F - (-1)^u W)\right. \\ &\quad + (F - (-1)^u N)(F - (-1)^u N)^T \\ &\quad + (E - (-1)^u F)^T (E - (-1)^u F) \\ &\quad \left. + (S - (-1)^u F)(S - (-1)^u F)^T\right]\left(3G^0 - G^1\right). \end{aligned} \quad (31)$$

B. Calculation of $MSDS_2$ in the Frequency Domain

Using (22), the expression $g_1 - g_2$, which is used for the calculation of the MSDS term ε_{nw} in (21), is found by

$$g_1 - g_2 = f(0, 0) - nw(7, 7) - \left(\frac{nw(7, 7) - nw(6, 6)}{2} + \frac{f(1, 1) - f(0, 0)}{2}\right). \quad (32)$$

The above may be expressed in the frequency domain, using (26) as

$$\begin{aligned} &g_1 - g_2 \\ &= \left(G_0^T F G^0 - G_7^T N W G^7\right) - \left(\frac{G_7^T N W G^7 - G_6^T N W G^6}{2} + \frac{G_1^T F G^1 - G_0^T F G^0}{2}\right). \end{aligned} \quad (33)$$

Using (28), (33) reduces to

$$g_1 - g_2 = \frac{3}{2} G_0^T (F - NW) G^0 - \frac{1}{2} G_1^T (F - NW) G^1. \quad (34)$$

Using (21), the MSDS term ε_{nw} is now easily computed. Likewise, similar expressions are found for ε_{ne}, ε_{sw}, and ε_{se}, and from (23) the expression of the MSDS_2 in the frequency domain is immediately obtained.

Fig. 5. Images used for the experimental evaluation of the proposed method. (a) 512 × 512 original "Lena" image. (b) 512 × 512 original "Peppers" image. (c) 512 × 512 original "Boat" image. (d) 512 × 512 original "Crowd" image. (e) 256 × 256 original "Moon" image. (f) 256 × 256 original "Couple" image. (g) 256 × 256 original "Girl" image. (h) 256 × 256 original "Pentagon" image. (i) 128 × 128 original "Claire" image. (k) First frame of the 352 × 240 original "Tennis" image sequence. (l) First frame of the 176 × 144 original "Foreman" image sequence.

C. Local Minimization of MSDS$_t$ for Each Frequency

We now set to zero all frequencies apart from frequency (k, l). This implies that we set to zero all elements of the DCT matrices involved in the expressions of MSDS_1 and MSDS_2 in the frequency domain, apart form the specific (k, l) element. Thus, for the computation of MSDS_1 using (31), we set to zero all elements with frequencies $(i, j) \neq (k, l)$ of the matrices F, W, E, S and N. If p_i is the ith element of the vector $(3G^0 - G^1)$, the MSDS_1^{kl} for the specific frequency (k, l) is now easily derived from (31) as follows:

$$\begin{aligned}\text{MSDS}_1^{kl} = \frac{1}{4}\,\big(&p_k^2(S_{k,l} - (-1)^k F_{k,l})^2 \\ &+ p_k^2(F_{k,l} - (-1)^k N_{k,l})^2 \\ &+ p_l^2(F_{k,l} - (-1)^k W_{k,l})^2 \\ &+ p_l^2(E_{k,l} - (-1)^k F_{k,l})^2\big) \qquad (35)\end{aligned}$$

where the subscripts k, l indicate the (k, l)th element of each matrix.

For MSDS$_2$, we also set to zero all frequencies apart from the frequency (k, l). Then, if $a_i = (G^0)_i$, $b_i = (G^1)_i$, and using (21) and (34), we obtain for the MSDS term ε_{nw}^{kl} computed only for the (k, l) frequency the following expression:

$$\varepsilon_{nw}^{kl} = \left(\frac{9}{4}a_k^2 a_l^2 - \frac{3}{2}a_k a_l b_k b_l + \frac{1}{4}b_k^2 b_l^2\right)[F_{k,l} - NW_{k,l}]^2. \tag{36}$$

For all four diagonal blocks, the MSDS$_2^{kl}$ for the specific frequency (k, l) is

$$\begin{aligned}\text{MSDS}_2^{kl} &= \varepsilon_{nw}^{kl} + \varepsilon_{ne}^{kl} + \varepsilon_{sw}^{kl} + \varepsilon_{se}^{kl} \\ &= \left(\frac{9}{4}a_k^2 a_l^2 - \frac{3}{2}a_k a_l b_k b_l + \frac{1}{4}b_k^2 b_l^2\right) \\ &\quad \cdot \left[(F_{k,l} - NW_{k,l})^2 + (SW_{k,l} - F_{k,l})^2 \right. \\ &\quad \left. + (SE_{k,l} - F_{k,l})^2 + (F_{k,l} - NE_{k,l})^2\right]. \end{aligned} \tag{37}$$

Setting the gradient of MSDS$_1^{kl}$ and MSDS$_2^{kl}$ to zero, we obtain the representation corresponding to the minimum MSDS$_t^{kl}$. Therefore, the imposition of

$$\frac{\partial(\text{MSDS}_t^{kl})}{\partial F_{k,l}} = \frac{\partial(\text{MSDS}_1^{kl} + \text{MSDS}_2^{kl})}{\partial F_{k,l}} = 0 \tag{38}$$

results in

$$\begin{aligned} &2(p_k^2 + p_l^2)F_{k,l} + 4RF_{k,l} \\ &\quad = (S_{k,l} + N_{k,l})(-1)^k p_k^2 + (W_{k,l} + E_{k,l})(-1)^k p_l^2 \\ &\qquad + (NW_{k,l} + NE_{k,l} + SW_{k,l} + SE_{k,l})R \end{aligned} \tag{39}$$

where $R = 9a_k^2 a_l^2 - 6a_k a_l b_k b_l + b_k^2 b_l^2$. Thus, (39) provides the expression of the DCT coefficient at frequency (k, l), as shown in (40), at the bottom of the page, subject to

$$F_{k,l}^L \le F_{k,l} \le F_{k,l}^U \tag{41}$$

where $F_{k,l}^U$ and $F_{k,l}^L$ are the quantization upper and lower limit, respectively.

Note that the proposed algorithm is developed in the frequency domain using DCT coefficients of the image. We chose however to use the Laplacian corrected DCT coefficients instead of the simple DCT reconstructed coefficients in the formula which provides the correction of the DCT coefficients, because the former are statistically better estimates of the original DCT coefficients.

Therefore, (40)—subject to the constraint of—(41) provides the correction of the (k, l) DCT coefficient for the reduction of the blocking effect in B-DCT coded images (e.g., JPEG coded images), in terms of its eight neighboring Laplacian corrected DCT coefficients in the subband-like domain. Fig. 4 shows the frequency response of the filter of (40) for the example frequencies $(k, l) = 2, 3$.

V. Experimental Results

In this section, simulation results demonstrating the performance of the proposed technique are presented. For this purpose, several images (as shown in Fig. 5) of different characteristics were chosen and compressed using a JPEG and MPEG-1 intra-picture. The same algorithm can be also applied for the case of MPEG inter-coding with no extra modifications.

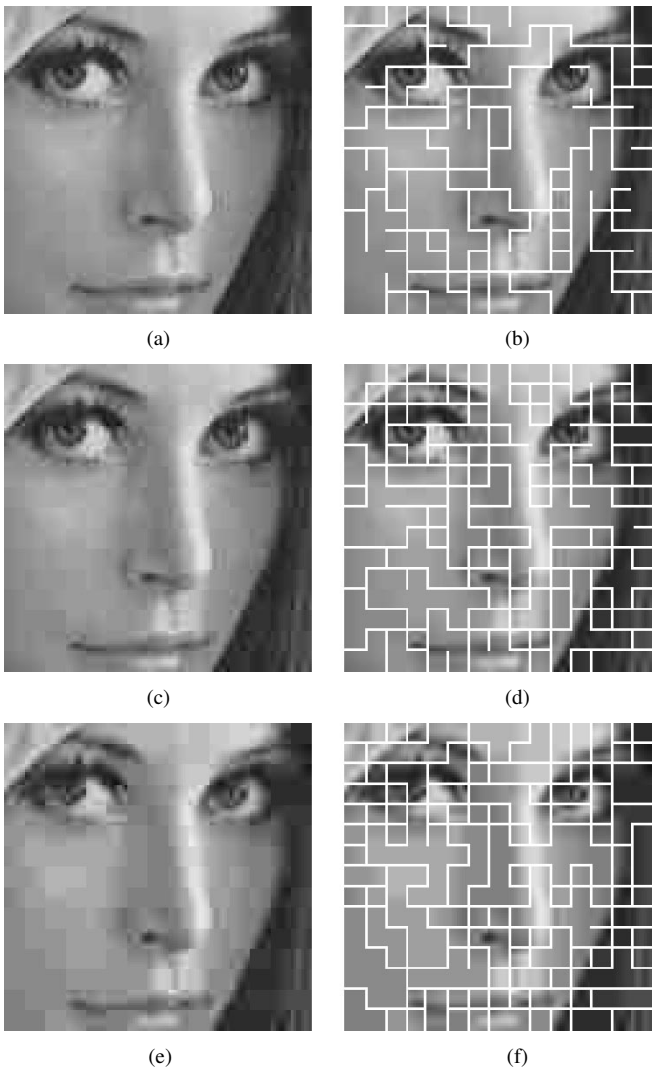

Fig. 6. (a) Portion of JPEG coded "Lena" image at 0.4096 bpp. (b) Detection of blocking artifacts at 0.4096 bpp. (c) Portion of JPEG coded "Lena" image at 0.2989 bpp. (d) Detection of blocking artifacts at 0.2989 bpp. (e) Portion of JPEG coded "Lena" image at 0.1942 bpp. (f) Detection of blocking artifacts at 0.1942 bpp.

The blocking artifact detection algorithm, presented in Section III, was applied to the test images, in order to locate the blocks affected by artifacts in a JPEG coded image. Figs. 6–8 show the disturbing blocking artifacts (indicated with a white pixel value) pointed out by the criterion (16) in the JPEG coded images at three different bit rates for the images of "Lena," "Peppers," and "Claire." In Figs. 6 and 7, magnified portions of the "Lena" and "Peppers" images are shown, so as to better illustrate the detection of the blocking artifacts. The portions used are identified by a white line in the "Lena" and "Peppers" original images (see Fig. 5).

In order to measure and evaluate the performance of our approach for blocking artifact reduction, the proposed constrained optimization method is applied to the test images of Fig. 5. Com-

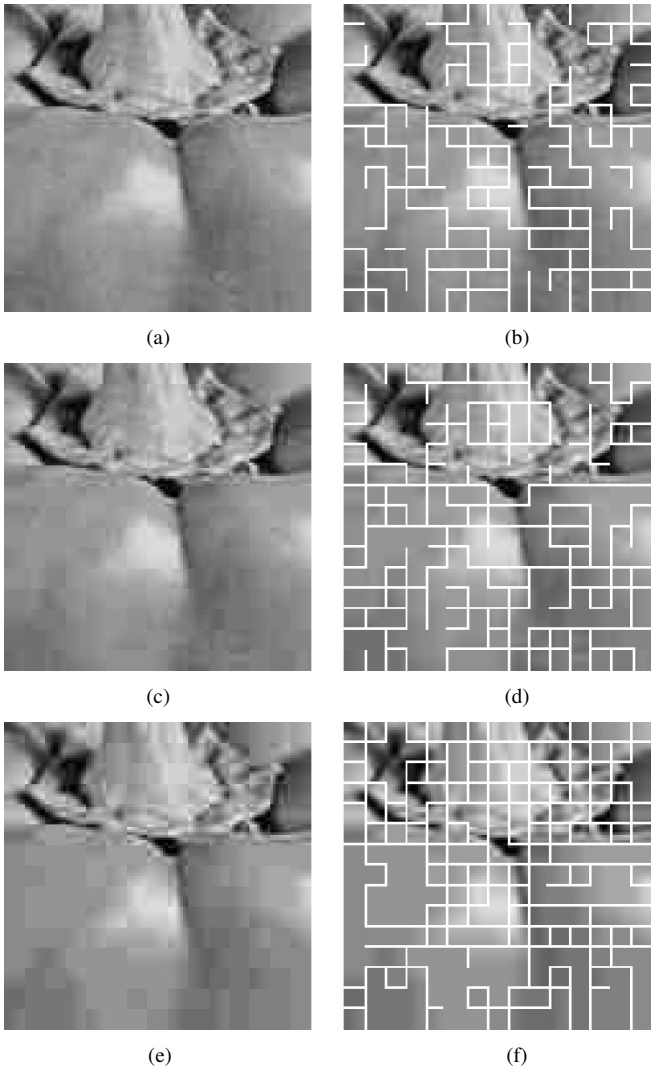

Fig. 7. (a) Portion of JPEG coded "Peppers" image at 0.4211 bpp. (b) Detection of blocking artifacts at 0.4211 bpp. (c) Portion of JPEG coded "Peppers" image at 0.3137 bpp, (d) Detection of blocking artifacts at 0.3137 bpp. (e) Portion of JPEG coded "Peppers" image at 0.1989 bpp. (f) Detection of blocking artifacts at 0.1989 bpp.

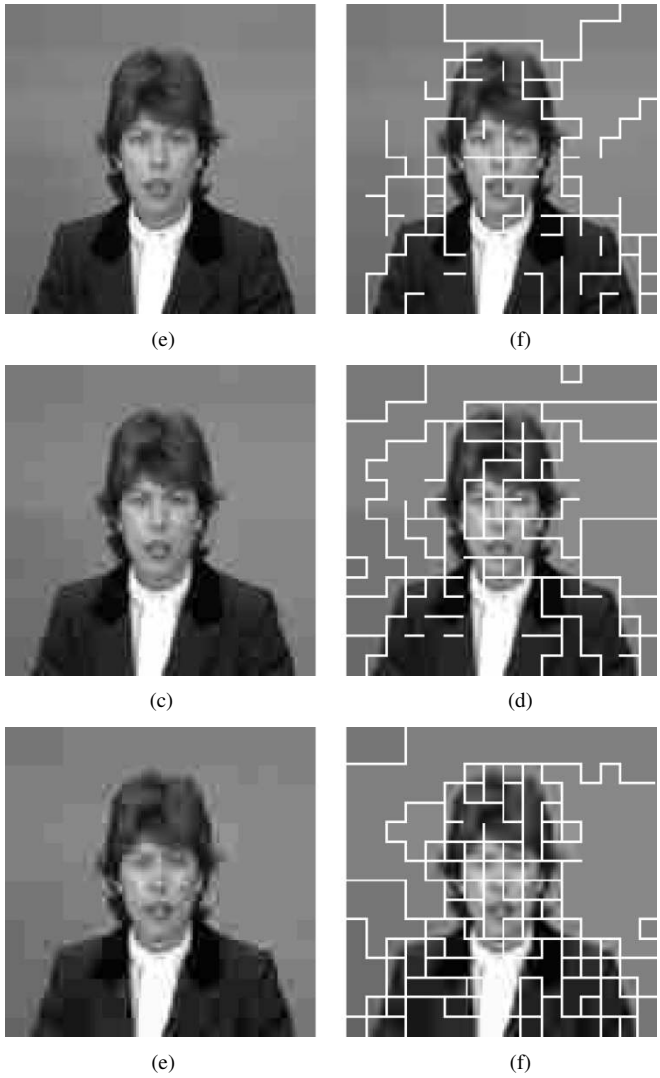

Fig. 8. (a) JPEG coded "Claire" image at 0.4907 bpp. (b) Detection of blocking artifacts at 0.4907 bpp. (c) JPEG coded "Claire" image at 0.3779 bpp. (d) Detection of blocking artifacts at 0.3779 bpp. (e) JPEG coded "Claire" image at 0.2968 bpp. (f) Detection of blocking artifacts at 0.2968 bpp.

monly used metrics, such as the mean square error or signal-to-noise ratio were not employed, since they involve pixels of the entire image and not just the pixels near the block boundaries. Rather, the value of the MSDS_t per block is preferred to be used for the evaluation of the proposed technique.

Recall that the recalculation of the DCT coefficients for blockiness removal is given in (40) and uses the Laplacian corrected DCT coefficients $\hat{F}_{ij}^{R}(u, v)$. This formula is produced after the minimization of the newly introduced formula of MSDS_t for each frequency separately. Furthermore, the blockiness reduction algorithm is applied only when criterion (16) is valid. This implies that the algorithm is performed only where disturbing blocking artifacts are expected to be present.

Table I shows the image name, its size, the MSDS_t of the original image (all in the first column), the coding rate (bits per pixel), and the MSDS_t per image block for the cases of: 1) the nonsmoothed reconstructed image; 2) the reconstructed image processed by method of [34]; and 3) the reconstructed image processed by the proposed algorithm. As expected, in B-DCT coded images, the value of MSDS_t per block increases compared to the original images, due to quantization. Our approach shows a significant reduction of the MSDS_t and clearly outperforms the method proposed in [34]. A visual illustration of the performance of our method, showing the JPEG reconstructed magnified portions of "Lena," "Peppers" and "Claire" images and the corresponding reconstructed portions of the images processed by the proposed method is shown in Fig. 9 and in more

$$F_{k,l} = \frac{(S_{k,l} + N_{k,l})(-1)^k p_k^2 + (W_{k,l} + E_{k,l})(-1)^k p_l^2 + (NW_{k,l} + NE_{k,l} + SW_{k,l} + SE_{k,l})R}{2(p_k^2 + p_l^2) + 4R} \tag{40}$$

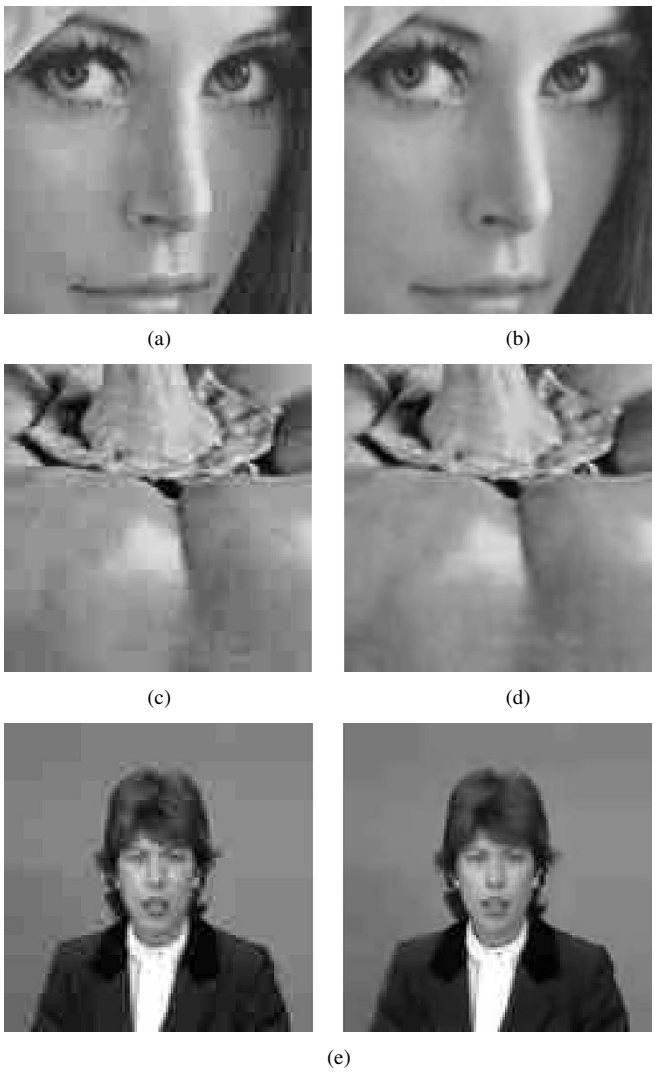

Fig. 9. (a) Portion of the JPEG coded "Lena" image at 0.2989 bpp. (b) Reduction of blocking artifacts with the proposed method at 0.2989 bpp. (c) Portion of the JPEG coded "Peppers" image at 0.3137 bpp. (d) Reduction of blocking artifacts with the proposed method at 0.3137 bpp. (e) JPEG coded "Claire" image at 0.3779 bpp. (f) Reduction of blocking artifacts with the proposed method at 0.3779 bpp.

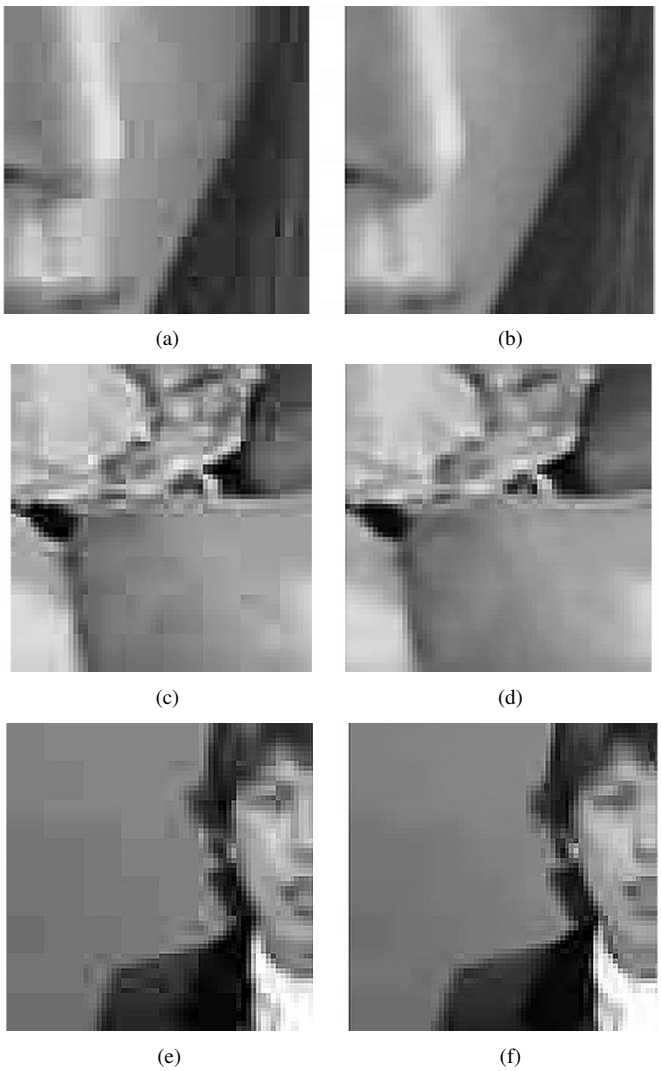

Fig. 10. (a) Portion of the JPEG coded "Lena" image at 0.2989 bpp. (b) Reduction of blocking artifacts with the proposed method at 0.2989 bpp. (c) Portion of the JPEG coded "Peppers" image at 0.3137 bpp. (d) Reduction of blocking artifacts with the proposed method at 0.3137 bpp. (e) Portion of the JPEG coded "Claire" image at 0.3779 bpp. (f) Reduction of blocking artifacts with the proposed method at 0.3779 bpp.

detail in Fig. 10. These figures illustrate the efficiency of the proposed method. Moreover, to better illustrate the comparison of the proposed method to the method in [34], the JPEG coded image "Lena" is used in Fig. 11.

Table II shows the results found when comparing the proposed method with the method of [34] using the metric of $MSDS_1$ (this metric is used in [34]). The metric of $MSDS_1$ (instead of $MSDS_t$) does not take into account the differences between the diagonal pixels. Thus, this metric is not suitable for evaluating the corner outliers reduction. However, the results indicate that the proposed algorithm continues to outperform the method of [34] since it uses the local optimization for every frequency separately, employs the corrected Laplacian DCT coefficients instead of the simple reconstructed DCT coefficients and involves more neighboring pixels (i.e., the diagonal pixels), producing better estimation of the recalculation of the DCT coefficients.

As stated earlier, the newly introduced form of $MSDS_t$ in the paper serves so as to remove the disturbing corner outliers from the reconstructed images. In order to better illustrate the effectiveness of the proposed method for the corner outlier reduction, Fig. 12 compares the results of the proposed method to the method of [34]. As is clear from this comparison, the algorithm of [34] reduces the blocking artifacts but fails to reduce the corner outliers, while the proposed algorithm succeeds to further reduce both the blocking artifacts and the corner outliers.

Tables III–V indicate the improvement achieved by the various innovations introduced in the present paper. This improvement is evaluated using three test images compressed at two different rates.

First, Table III compares the $MSDS_t$ of the proposed method which uses the Laplacian corrected DCT coefficients for the recalculation of the DCT coefficients and the $MSDS_t$ of the method which employs the simple reconstructed DCT coefficients instead. Both methods employ the local minimization of the $MSDS_t$ form and use the prior blockiness detection method. Results clearly show that the contribution of the introduction of the Laplacian corrected DCT coefficients in our method is significant.

(a) (b) (c)

Fig. 11. (a) Detail of the JPEG coded image Lena at 0.2989 bpp. (b) Same detail as the image processed by the method of [34]. (c) Same detail as the image processed by the proposed method.

TABLE I
$MSDS_t$ PER BLOCK FOR VARIOUS TEST IMAGES

original image	bit per pixel	$MSDS_t$ of the nonsmoothed reconstructed image	$MSDS_t$ of the reconstructed image processed by method [34]	$MSDS_t$ of the reconstructed image processed by proposed method
lenna	0.4096 bpp	3118	2980	2512
512 × 512	0.2989 bpp	3898	3397	2790
$MSDS_t$=1608	0.1942 bpp	5413	4976	4012
peppers	0.4211 bpp	2513	2311	2023
512 × 512	0.3137 bpp	3013	2798	2455
$MSDS_t$=2341	0.1989 bpp	4467	3877	3184
boat	0.4988 bpp	6145	5844	5001
512 × 512	0.3245 bpp	7539	7008	6332
$MSDS_t$=4393	0.2417 bpp	8489	7823	6802
crowd	0.4811 bpp	5611	5212	5001
512 × 512	0.3528 bpp	7288	6788	6420
$MSDS_t$=1968	0.2936 bpp	8347	7899	7200
moon	0.3469 bpp	3617	3509	3317
256 × 256	0.2589 bpp	3792	3580	3401
$MSDS_t$=3172	0.1571 bpp	4014	3881	3550
couple	0.3688 bpp	3847	3789	3512
256 × 256	0.2832 bpp	4105	3908	3788
$MSDS_t$=2393	0.1879 bpp	4967	4640	4145
girl	0.4701 bpp	3782	3455	3013
256 × 256	0.3303 bpp	4709	4344	3979
$MSDS_t$=2220	0.2325 bpp	6386	5601	5003
pentagon	0.5923 bpp	7905	7677	6990
256 × 256	0.3989 bpp	8910	8672	7899
$MSDS_t$=6235	0.2944 bpp	9886	9390	8674
claire	0.4907 bpp	3387	3012	2679
128 × 128	0.3779 bpp	3762	3459	2891
$MSDS_t$=1282	0.2968 bpp	4805	4112	3550
foreman (1st frame)	0.5918 bpp	3633	3501	3109
176 × 144	0.3945 bpp	3900	3782	3233
$MSDS_t$=2913	0.2761 bpp	4423	3989	3412
tennis (1st frame)	0.5073 bpp	2540	2411	2101
352 × 240	0.3382 bpp	3021	2846	2261
$MSDS_t$=1769	0.1691 bpp	3809	3519	2910

Table IV also compares the $MSDS_t$ of two methods. The first method uses the local minimization of the $MSDS_t$ form while the second uses the local minimization of the $MSDS_1$ form. Both methods employ the Laplacian corrected DCT coefficients for the DCT recalculation and the prior blockiness detection method. Results show that the use of $MSDS_t$ for the DCT recalculation provides better results than the use of the simple form of $MSDS_1$.

Finally, Table V illustrates the results for the $MSDS_t$ when we employ the separate for each frequency minimization of $MSDS_t$ compared to the results produced when we apply the global minimization of $MSDS_1$. In both methods, the corrected Laplacian corrected DCT coefficients and the prior blockiness detection method are used. Results clearly support and justify our choice to use the separate for each frequency minimization of $MSDS_t$ for the DCT recalculation.

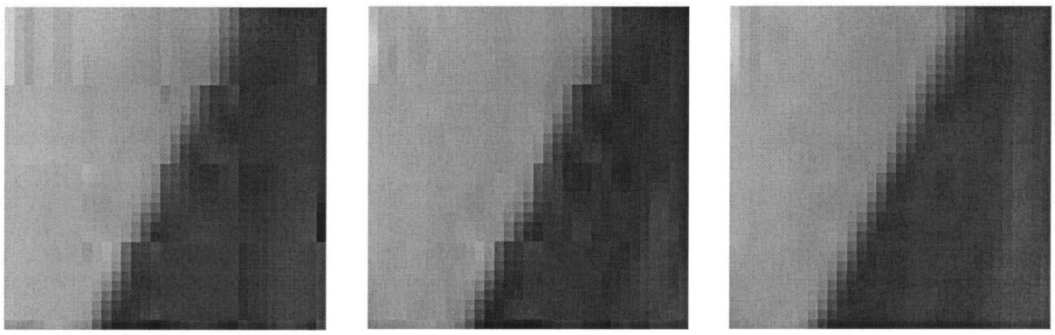

(a) (b) (c)

Fig. 12. (a) Detail of the JPEG coded image Lena at 0.2989 bpp with corner outliers. (b) Same detail of the image processed by the method of [34]. (c) Same detail of the image processed by the proposed method.

TABLE II
$MSDS_1$ PER BLOCK FOR THREE TEST IMAGES

original image	bit per pixel	$MSDS_1$ of the nonsmoothed reconstructed image	$MSDS_1$ of the reconstructed image processed by method [34]	$MSDS_1$ of the reconstructed image processed by proposed method
lenna	0.4096 bpp	2422	2359	2121
512 × 512	0.2989 bpp	2881	2607	2312
$MSDS_1$=1246	0.1942 bpp	4297	3911	3467
peppers	0.4211 bpp	1971	1802	1633
512 × 512	0.3137 bpp	2392	2207	2001
$MSDS_1$=2009	0.1989 bpp	3580	3060	2587
claire	0.4907 bpp	2650	2347	2261
128 × 128	0.3779 bpp	2968	2669	2421
$MSDS_1$=931	0.2968 bpp	3800	3175	2841

TABLE III
$MSDS_t$ PER BLOCK FOR THREE TEST IMAGES WHEN WE APPLY THE PROPOSED METHOD WITH OR WITHOUT USING THE CORRECTED LAPLACIAN DCT COEFFICIENTS

original image	bit per pixel	proposed method **without** the use of the Laplacian corrected DCT coefficients	proposed method **with** the use of the Laplacian corrected DCT coefficients
lenna	0.4096 bpp	2608	2512
512 × 512	0.2989 bpp	2892	2790
$MSDS_t$=1608	0.1942 bpp	4237	4012
peppers	0.4211 bpp	2110	2023
512 × 512	0.3137 bpp	2575	2455
$MSDS_t$=2341	0.1989 bpp	3319	3184
claire	0.4907 bpp	2743	2679
128 × 128	0.3779 bpp	2989	2891
$MSDS_t$=1282	0.2968 bpp	3719	3550

The blocking artifact reduction algorithm is somewhat slower than the algorithm in [34], since it employs the Laplacian corrected DCT coefficients and involves the diagonal adjacent pixels. However, the overall proposed algorithm was found to be faster than that of [34] because of the use of the blockiness detection algorithm which excludes the blocks where the blocking artifacts are not disturbing (especially at high bit rates). Table VI shows the time needed in order to apply our algorithm compared to the algorithm of [34]. Note that larger values of the coding rate indicate that the blockiness reduction algorithm will be applied in fewer blocks, since there will not be many disturbing blocking artifacts and as a result the proposed algorithm will be faster.

Furthermore, the proposed algorithm is applied on the received/reconstructed DCT coefficients and, therefore, does not need extra time for pixel postprocessing needed by methods

TABLE IV
$MSDS_t$ PER BLOCK FOR THREE TEST IMAGES WHEN WE APPLY THE PROPOSED METHOD USING THE LOCAL MINIMIZATION OF $MSDS_1$ OR $MSDS_t$

original image	bit per pixel	proposed method using the local minimization of $\mathbf{MSDS_1}$	proposed method using the local minimization of $\mathbf{MSDS_t}$
lenna	0.4096 bpp	2698	2512
512 × 512	0.2989 bpp	3091	2790
$MSDS_t$=1608	0.1942 bpp	4349	4012
peppers	0.4211 bpp	2177	2023
512 × 512	0.3137 bpp	2661	2455
$MSDS_t$=2341	0.1989 bpp	3463	3184
claire	0.4907 bpp	2838	2679
128 × 128	0.3779 bpp	3153	2891
$MSDS_t$=1282	0.2968 bpp	3761	3550

TABLE V
$MSDS_t$ PER BLOCK FOR THREE TEST IMAGES WHEN WE APPLY THE THREE PROPOSED METHOD USING THE GLOBAL MINIMIZATION OF $MSDS_1$ OR THE LOCAL MINIMIZATION OF $MSDS_t$

original image	bit per pixel	proposed method using the **global** minimization of $MSDS_1$	proposed method using the **local** minimization of $MSDS_t$
lenna	0.4096 bpp	2868	2512
512 × 512	0.2989 bpp	3261	2790
$MSDS_t$=1608	0.1942 bpp	4795	4012
peppers	0.4211 bpp	2269	2023
512 × 512	0.3137 bpp	2711	2455
$MSDS_t$=2341	0.1989 bpp	3719	3184
claire	0.4907 bpp	2910	2679
128 × 128	0.3779 bpp	3344	2891
$MSDS_t$=1282	0.2968 bpp	3981	3550

TABLE VI
TIME NEEDED TO APPLY THE PROPOSED ALGORITHM COMPARED TO THE TIME NEEDED TO APPLY THE ALGORITHM OF [34] AND THE MPEG-4 DEBLOCKING FILTER. THE VALUE OF t FOR A 512 × 512 IMAGE IS 0.29 MS ON A PENTIUM III BASED PC. THE PROPOSED ALGORITHM FIRST EMPLOYS THE PROPOSED BLOCKINESS DETECTION SCHEME

original image	bit per pixel	time needed with the method of [34]	time needed with the MPEG-4 deblocking filter	time needed with the proposed method
lenna	0.4096 bpp	t	8.79*t	0.73*t
512 × 512	0.2989 bpp	t	8.80*t	0.87*t
$MSDS_t$=1608	0.1942 bpp	t	8.82*t	0.94*t
peppers	0.4211 bpp	t	8.80*t	0.75*t
512 × 512	0.3137 bpp	t	8.83*t	0.85*t
$MSDS_t$=2341	0.1989 bpp	t	8.85*t	0.92*t

applied in the spatial domain. Thus, it is much faster than methods working in the spatial domain. Compared, for example, with the well-known spatial domain deblocking method of the MPEG-4 postfilter [42], our algorithm is about nine times faster (see Table VI).

VI. Conclusions

When images are compressed using B-DCT transforms, the decompressed images often contain bothersome blocking artifacts. This paper presented a novel algorithm applied entirely in the compressed domain, in order to detect and reduce these blocking artifacts. In our approach, the Laplacian statistical model is adopted for the DCT coefficients and a better estimation of the DCT reconstructed coefficients is produced, in order to calculate the relative theoretical quantization error. This error is used in a newly introduced criterion, in order to efficiently detect the blocking artifacts of coded images. Thus, the time and the computational load of the deblocking algorithm is reduced compared to other deblocking methods, since it is applied only where is needed. A novel form of the criterion of MSDS (i.e., the MSDS_t form) is also introduced involving all eight neighboring blocks, instead of the simple form of MSDS which [34] uses. MSDS_t is then minimized for each frequency separately, producing a closed form for the correction terms for the DCT coefficients so as to achieve reduction of the blocking effect of coded images. This local minimization is shown to achieve better results than the global minimization adopted in [34]. Experimental evaluation of the performance of the proposed technique showed its ability to detect and alleviate blocking artifacts effectively.

References

[1] W. B. Pennebaker and J. L. Mitchel, *JPEG Still Image Data Compression Standard*. New York: Van Nostrand, 1993.

[2] G. K. Wallace, "The JPEG still-picture compression standard," *Commun. ACM*, vol. 34, pp. 30–44, Apr. 1991.

[3] *Video Coding for Low Bit Rate Communications*, ITU-T Telecommunications Standardization Sector, Recommendation H.263, ver. 2, Jan. 1998.

[4] K. R. Rao and J. J. Hwang, *Techniques and Standards for Image, Video, and Audio Coding*, NJ: Prentice Hall, 1996.

[5] H. S. Malvar and D. H. Staelin, "The LOT: Transform coding without blocking effects," *IEEE Trans. Accoust., Speech, Signal Processing*, vol. 37, pp. 553–559, 1989.

[6] H. S. Malvar, "Biorthogonal and nonuniform lapped transforms for transform coding with reduced blocking and ringing artifacts," *IEEE Trans. Signal Processing*, vol. 46, pp. 1043–1053, Apr. 1998.

[7] T. Jarske, P. Haavisto, and I. Defe'e, "Post-filtering methods for reducing blocking effects from coded images," *IEEE Trans. Consumer Electron.*, pp. 521–526, Aug. 1994.

[8] H. C. Reeve and J. S Lim, "Reduction of blocking artifacts in image coding," *Opt. Eng.*, vol. 23, pp. 34–37, Jan./Feb. 1984.

[9] T. Meier, K. N. Ngan, and G. Crebbin, "A region-based algorithm for enhancement of images degraded by blocking effects," in *Proc. IEEE Tencon'96*, vol. 1, Perth, Australia, Nov. 1996, pp. 405–408.

[10] J. G. Apostolopoulos and N. S. Jayant, "Postprocessing for low bit-rate video compression," *IEEE Trans. Image Processing*, vol. 8, pp. 1125–1129, Aug. 1999.

[11] R. Molina, A. K. Katsaggelos, and J. Abad, "Bayesian image restoration using a wavelet-based subband decomposition," in *Proc. 1999 Int. Conf. Acoust., Speech, Signal Processing*, Phoenix, AZ, Mar. 15–19, 1999.

[12] Z. Xiong, M. T. Orchard, and Y. Q. Zhang, "A deblocking algorithm for JPEG compressed images using overcomplete wavelet representations," *IEEE Trans. Circuits Syst. Video Technology*, vol. 7, pp. 692–695, Aug. 1999.

[13] N. C. Kim, I. H. Jang, D. H. Kim, and W. H. Hong, "Reduction of blocking artifact in block-coded images using wavelet transform," *IEEE Trans. Circuits Syst. Video Technology*, vol. 8, pp. 253–257, June 1998.

[14] T.-C. Hsung, D. P. K. Lun, and W.-C. Siu, "A deblocking technique for block-transform compressed image using wavelet transform modulus maxima," *IEEE Trans. Image Processing*, vol. 7, pp. 1488–1496, Oct. 1998.

[15] T. P Rourke and R. L Stevenson, "Improved image decompression for reduced transform coding artifacts," *IEEE Trans. Circuits Syst. Video Technol.*, vol. 5, pp. 490–499, Dec. 1995.

[16] J. Luo, C. W. Chen, K. J. Parker, and T. S. Huang, "Artifact reduction in low bit rate DCT-based image compression," *IEEE Trans. Image Processing*, vol. 5, pp. 1363–1368, Sept. 1996.

[17] T. Meier, K. N. Ngan, and G. Crebbin, "Reduction of blocking artifacts in image and video coding," *IEEE Trans. Circuits Syst. Video Technology*, vol. 9, pp. 490–500, Apr. 1999.

[18] Y. Yang, N. P Galatsanos, and A. K. Katsaggelos, "Regularized reconstruction to reduce blocking artifacts of block discrete cosine transform compressed images," *IEEE Trans. Circuits Syst. Video Technol.*, vol. 3, pp. 421–423, Dec. 1993.

[19] ——, "Projection-based spatially adaptive reconstruction of block-transform compressed images," *IEEE Trans. Image Processing*, vol. 4, pp. 896–908, July 1995.

[20] K. May, T. Stathaki, A. Constantinides, and A. K. Katsaggelos, "Iterative determination of local bound constraints in iterative image restoration," in *Proc. 1998 IEEE Int. Conf. Image Processing*, vol. 2, Chicago, IL, Oct. 5–7, 1998, pp. 833–837.

[21] A. Zakhor, "Iterative procedures for reduction of blocking effects in transform image coding," *IEEE Trans. Circuits Syst. Video Technol.*, vol. 2, pp. 91–95, Mar. 1992.

[22] K. H. Tzou, "Post-filtering of transform-coded images," in *Proc. SPIE Applications of Digital Image Processing XI*, San Diego, CA, Aug. 1988.

[23] B. Ramamurthi and A. Gersho, "Nonlinear space-variant postprocessing of block coded images," *IEEE Trans. Accoust., Speech, Signal Processing*, vol. ASSP-34, pp. 1258–1268, Oct. 1986.

[24] Y.-F. Hsu and Y.-C. Chen, "A new adaptive separable median filter for removing blocking effects," *IEEE Trans. Consumer Electron.*, pp. 510–513, Aug. 1993.

[25] D. G. Sampson, D. V. Papadimitriou, and C. Chamzas, "Post-processing of block-coded Images at Low Bitrates," in *Proc. 1996 IEEE Int. Conf. Image Processing*, Lausanne, Switzerland, Sept. 1996.

[26] Y. L. Lee, H. C. Kim, and H. W. Park, "Blocking effect reduction of JPEG images by signal adaptive filtering," *IEEE Trans. Image Processing*, vol. 7, pp. 229–234, Feb. 1998.

[27] J. Chou, M. Crouse, and K. Ramchadran, "A simple algorithm for removing blocking artifacts in block transform coded images," *IEEE Signal Processing Lett.*, vol. 5, pp. 33–35, Feb. 1998.

[28] M. G. Strintzis, "Optimal construction of filter banks for subband coding of quantized signals," *Signal Processing Mag.*, vol. 62, pp. 15–36, 1997.

[29] ——, "Optimal pyramidal and subband decompositions for hierarchical coding of noisy and quantized images," *IEEE Trans. Image Processing*, vol. 7, pp. 155–167, Feb. 1988.

[30] M. G. Strintzis and D. Tzovaras, "Optimal pyramidal decomposition for progressive multi-dimensional signal coding using optimal quantizers," *IEEE Trans. Signal Processing*, vol. 46, pp. 1054–1069, Apr. 1998.

[31] H. Paek, R.-C. Kim, and S.-U. Lee, "On the POCS-based postprocessing technique to reduce the blocking artifacts in transform coded images," *IEEE Trans. Circuits Syst. Video Technol.*, vol. 8, pp. 358–367, June 1998.

[32] ——, "A DCT-based spatially adaptive post processing technique to reduce the blocking artifacts in transform coded images," *IEEE Trans. Circuits Syst. Video Technol.*, vol. 10, pp. 36–41, Feb. 2000.

[33] S. Minami and A. Zakhor, "An optimization approach for removing blocking effects in transform coding," *IEEE Trans. Circuits Syst. Video Technol.*, vol. 5, pp. 74–82, Apr. 1995.

[34] G. Lakhani and N. Zhong, "Derivation of prediction equations for blocking effect reduction," *IEEE Trans. Circuits Syst. Video Technol.*, vol. 9, pp. 415–418, Apr. 1999.

[35] K. R. Rao and P. Yip, *Discrete Cosine Transform: Algorithms, Advantages, Applications*. New York: Academic, 1990.

[36] A. Gersho and R. M. Gray, *Vector Quantization and Signal Compression*. Boston, MA: Kluwer, 1992.

[37] R. L. de Queiroz, "Processing JPEG-compressed images and documents," *IEEE Trans. Image Processing*, vol. 7, pp. 1661–1672, Dec. 1998.

[38] N. M. Namazi, P. Penafiel, and C. M. Fan, "Nonuniform image motion estimation using the Kalman filtering," *IEEE Trans. Image Processing*, vol. 3, pp. 678–683, Sept. 1994.
[39] K. E. Matthews and N. M. Namazi, "A Bayes decision test for detecting uncovered-background and moving pixels in image sequence," *IEEE Trans. Image Processing*, vol. 7, pp. 720–728, May 1998.
[40] N. M. I-Ming Pao and N. M. Ming-Ting Sun, "Modeling DCT coefficients for fast video encoding," *IEEE Trans. Circuits Syst. Video Technol.*, vol. 9, pp. 608–616, June 1999.
[41] A. K. Jain, *Fundamentals of Digital Image Processing*. Englewood Cliffs, NJ: Prentice-Hall, 1989.
[42] ISO/IEC/SC29/WG11, *Information Technology—Generic Coding of Audio-Visual Objects—Part 2: Visual ISO/IEC 14 496*, July 1999.

George A. Triantafyllidis (S'96) was born in Thessaloniki, Greece, in 1975. He received the diploma degree in 1997 from the Electrical Engineering Department, Aristotle University of Thessaloniki, Thessaloniki, Greece, where he is currently working toward the Ph.D. degree in the Information Processing Laboratory.

He is a Research Associate with Aristotle University of Thessaloniki. He has participated in several research projects funded by the European Union and the Greek Secretariat of Research and Technology. Since 2000, he has served as a Teaching Assistant at Aristotle University of Thessaloniki. His research interests include image compression and analysis, as well as monoscopic and stereoscopic image sequence coding and processing.

Dimitrios Tzovaras received the diploma degree in electrical engineering and the Ph.D. degree in 2-D and 3-D image compression from Aristotle University of Thessaloniki, Thessaloniki, Greece, in 1992 and 1997, respectively.

He is a now Researcher in the Informatics and Telematics Institute of Thessaloniki. Previously, he was a Leading Researcher on 3-D imaging at Aristotle University of Thessaloniki. His main research interests include image compression, 3-D data processing, virtual reality, medical image communication, 3-D motion estimation, and stereo and multiview image sequence coding. His involvement with those research areas has led to the co-authoring of more than 20 papers in refereed journals and more than 50 papers in international conferences. Since 1992, he has been involved in more than 20 projects in Greece, funded by the European Commission, and the Greek Ministry of Research and Technology.

Dr. Tzovaras has served as a regular reviewer for a number of international journals and conferences. He is a member of the Technical Chamber of Greece.

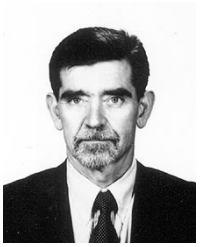

Michael Gerassimos Strintzis (S'68–M'70–SM'79) received the diploma degree in electrical engineering from the National Technical University of Athens, Athens, Greece, in 1967, and the M.A. and Ph.D. degrees in electrical engineering from Princeton University, Princeton, NJ, in 1969 and 1970, respectively.

He then joined the Electrical Engineering Department, University of Pittsburgh, Pittsburgh, PA, where he served as Assistant Professor (1970–1976) and Associate Professor (1976–1980). Since 1980, he has been Professor of Electrical and Computer Engineering at the University of Thessaloniki, Thessaloniki, Greece, and, since 1999, Director of the Informatics and Telematics Research Institute, Thessaloniki. His current research interests include 2-D and 3-D image coding, image processing, biomedical signal and image processing, and DVD and Internet data authentication and copy protection.

Dr. Strintzis has served as Associate Editor for the IEEE TRANSACTIONS ON CIRCUITS AND SYSTEMS FOR VIDEO TECHNOLOGY since 1999. In 1984, he was awarded a Centennial Medal of the IEEE.